

MPPT Control of a Small PV Generation System under Diverse Weather Conditions

F. Brihmat
 National Superior Polytechnic School,
 10 Hassen Badi avenue, P.C. 182, El Harrach,
 Algiers, Algeria,
 e.mail: fouzia_brihmat@yahoo.fr

S. Mekhtoub
 Electrotechnic Research Laboratory, 'LRE'
 National Superior Polytechnic School,
 10 Hassen Badi avenue, P.C. 182, El Harrach,
 Algiers, Algérie,
 e.mail: said.mekhtoub@enp.edu.dz
saidmekhtoub@yahoo.fr

Abstract— The power induced in the photovoltaic modules is influenced by the intensity of solar cell irradiation, temperature of solar cells and moreover by the load. Therefore, to maximize the efficiency of the renewable energy system, it is necessary to track the maximum power point of the input source. In this work, we tie to present the constituent of a weak power PV chain dedicated to the storage on battery. The battery bank is connected to the DC network via a DC/DC boost converter, called the storage converter, used for controlling the network. Indeed, the battery is only imperative buffer storage in this case. The PV units are connected to the DC network via its own DC/DC converter, called PV converter, to ensure the required power flow.

The purpose of the proposed model is the simulation of the complete system behavior from the electric and energy point of view. A maximum power point tracker (MPPT) scheme is applied through the boost converter to improve the energy conversion efficiency. Fuzzy algorithm based on linguistic rules describing the operator's control strategy is applied to control the step-up converter for MPPT. On the other hand, Fuzzy logic control based on coarse and fine mode is incorporated in order to reduce not only the time required to track the maximum power point but also power fluctuation. A confrontation with a P and O method performed. Another fuzzy battery-charge controller is also applied.

Simulation results show that the proposed fuzzy controller exhibits a better performance than the controller based upon the P and O method.

Keywords — Photovoltaic; Simulation; MPPT; DC-DC converter; Fuzzy controller

I. INTRODUCTION

Solar power is a renewable energy source that might one day soon replace fossil fuel dependent energy sources. However, for that to happen, solar power cost per kilowatt-hour has to be competitive with fossil fuel energy sources. Currently, solar panels are not very efficient with only about 12 ~ 20% efficiency in their ability to convert sunlight to electrical power. The efficiency can drop further due to other factors such as solar panel temperature and load conditions. In order to maximize the power derived from the solar panel it is important to operate the panel at its optimal power point. To

achieve this, a type of charge controller called a Maximum Power Point Tracker will be designed and implemented. Nowadays, the available application area and the installation of PV system are rapidly growing by a number of factors such as global warming, energy security, technology improvements and decreasing costs. In particular, stand-alone PV generation systems are attractive and indispensable electricity source for the security camera devices, streetlights, electric signs and weather observation systems where some of them may be placed in remote or mountainous locations [1].

II. PHOTOVOLTAIC SYSTEM

Fig. 1 shows the block diagram of autonomous photovoltaic system. The latter consists of the following elements:

- A photovoltaic panel;
- A DC-DC converter Boost-type;
- Battery as a load;
- And an MPPT controller.

A. Modeling of the photovoltaic system

The closest electric model to photovoltaic generator is a model with two diodes with different form factors and different laws of behavior compared to temperature, see Fig.1.

Fig. 2 is a representation of the mathematical model for the current-voltage characteristic given by [2];

$$i = i_{ph} - i_{s1} \left[e^{\frac{q(v+i.r_s)}{n_1 k T}} - 1 \right] - i_{s2} \left[e^{\frac{q(v+i.r_s)}{n_2 k T}} - 1 \right] - \frac{v+i.r_s}{r_{sh}} \quad (1)$$

i_{s1} and i_{s2} are the saturation currents of the diodes, n_1 and n_2 their purity factors. The photocurrent $i_{ph.max}$ is reached at a maximum insolation, often we have ($i_{ph} = S_i \cdot i_{ph.max}$) with S_i : percentage of insolation.

It is clear from equation (1), the current-voltage characteristic is strongly dependent on the insolation and temperature. The temperature dependence is further amplified by the properties of the photocurrent i_{ph} and the reverse saturation currents of the diodes which are given by HANNES [3]:

$$i_{ph}(T) = i_{ph}|_{(T=298.K)} \left[1 + (T - 298.K) \cdot (5 \cdot 10^{-4}) \right] \quad (2)$$

$$i_{d1} = k_1 T^3 e^{-\frac{E_g}{kT}} \quad (3)$$

$$i_{d2} = k_2 T^2 e^{-\frac{E_g}{kT}} \quad (4)$$

$$k_1 = 1,2 \left[A/cm^2 \cdot K^3 \right] \quad (5)$$

$$k_2 = 2,9 \cdot 10^5 \left[A/cm^2 \cdot K^{5/2} \right] \quad (6)$$

E_g is the energy band of the semiconductor.

B. Study of solar passive system

The solar passive system is a solar system without a regulator. It includes the following elements:

- 06 solar modules in parallel, each module containing 36 cells in series;
- A load formed by 02 of lead-acid batteries in series, each battery has an operating voltage of 12 V.

The purpose of this study is to see the behavior of the PV generator to regulate it to better use by extracting the maximum power.

First, the effect of irradiation on current-voltage characteristic of the photovoltaic panel, and the corresponding output power is represented on Fig. 3; We note that sunlight affects much more current I of the generator than its voltage.

In Fig. 4 is shown the current-voltage characteristic of the photovoltaic panel, and the corresponding output power under different temperature values

III. CONTROL OF ENERGY

The electric intensity provided by these modules depend, among other things, of the irradiation, their position to the sun, temperature and aging ... Where an irregularity in the supply of energy which may not be consistent with energy requirements, generally more constant. It is often necessary to control the supply of electricity by means of a system of energy storage and regulation of the stock. Sometimes it is also necessary to change the nature of power for some applications (converting DC to AC using an inverter). In what

follows we will detail the part of the operation of DC/DC converters, to ensure proper control [4].

A. DC/DC converter

Stand-alone photovoltaic systems are designed to be totally self-sufficient in generating, storing and supplying electricity to local electrical loads. The management of the energy flow within the system is performed through a regulation process.

The choppers are static DC/DC converters to generate a variable DC voltage source from a fixed source of DC voltage. The chopper consists of capacitors, inductors and switches. All these devices in the ideal case do not consume power, this is the reason why the choppers have good yields. Usually the switch is a MOSFET transistor which is a semiconductor device in (block-saturated) mode [5]. If the semiconductor device is blocked, the current is zero where the power dissipation is zero. If the device is in the saturated state, the voltage drop across its terminals is almost zero and consequently the power loss will be very small [6].

As shown in Fig. 5 for the operation of the chopper, the switch is closed with a closure time equal to $\alpha \cdot T_s$, and opened in an opening time = $(1-\alpha)T_s$, where:

- T_s is the switching period equals to $1/f_s$.
- α the duty cycle of the switch ($\alpha \in [0,1]$).

In this section we will discuss about the different types of DC/DC converters in order to model them mathematically for an easy use of simulation.

The lead-acid batteries are currently the only acceptable sets from investment and cost operation viewpoint [7].

For this, optimization by means of an MPPT (Maximum Power Point Tracking) is more than necessary.

A. Battery bank

The solar power outputs can fluctuate on an hourly or daily basis. The stand-alone system must, therefore, have some means of storing energy, which can be used later to supply the load during the periods of low or no power output.

Fig. 6 shows the general structure of a battery. It is represented by four blocks:

- Capacity block;
- Voltages block;
- State of the charge block (SOC);
- Gassing current losses block.

IV. MAXIMUM POWER POINT TRACKER (MPPT)

The maximum power that corresponds to the optimal operating point is determined for different sunburn of sunlight, as well as different variations of temperature. DC/DC converter type is used in the control part of the photovoltaic system because it is easy to control by its duty cycles using a PWM (Pulse Width Modulation) signal. Here, Boost chopper is used as an interface power to control by MPPT controller to

adapt the output voltage of the chopper to the voltage required by the load. From this rule and the type of controller, we may reason about several different methods to extract the maximum power from a solar panel. Some of the concepts are very robust and simple, while other approaches require very sophisticated logic devices such as microprocessors combined with power circuits, switching converters ... In this paper we propose a fuzzy logic-based concept. More than thirty methods of continuing MPP had been proposed, but the most prominent is the famous P&O (Perturbe and Observe) algorithm that predominates.

A. Perturb & Observe Method

Perturb & Observe (P&O) is the simplest method. In this we use only one sensor, that is the voltage sensor, to sense the PV array voltage and so the cost of implementation is less and hence easy to implement. The time complexity of this algorithm is very less but on reaching very close to the MPP it doesn't stop at the MPP and keeps on perturbing on both the directions. When this happens the algorithm has reached very close to the MPP and we can set an appropriate error limit or can use a wait function which ends up increasing the time complexity of the algorithm.

However the method does not take account of the rapid change of irradiation level (due to which MPPT changes) and considers it as a change in MPP due to perturbation and ends up calculating the wrong MPP. To avoid this problem we can use incremental conductance method.

Fig. 7 shows the flowchart of the algorithm for P & O as it should be implemented in the control microprocessor.

B. MPPT based on fuzzy logic

Basically, the difficult task of modeling and simulating complex real-world systems for control systems development, especially when implementation issues are considered, is well documented of some motivations for turning to fuzzy control.

Fundamentally, the fuzzy controller should be viewed as an artificial decision maker that operates in a closed-loop system in real time. It gathers plant output data, compares it to the reference input, and then decides what the plant input should be to ensure that the performance objectives will be met.

It has four main components: (1) The "rule-base" holds the knowledge, in the form of a set of rules, of how best to control the system. (2) The inference mechanism evaluates which control rules are relevant at the current time and then decides what the input to the plant should be. (3) The fuzzification interface simply modifies the inputs so that they can be interpreted and compared to the rules in the rule-base. And (4) the defuzzification interface converts the conclusions reached by the inference mechanism into the inputs to the plant. Its basic structure is illustrated on Fig. 8;

These two variables are defined as follows:

$$E(k_s) = \frac{P_{ph}(k_s) - P_{ph}(k_s - 1)}{V_{ph}(k_s) - V_{ph}(k_s - 1)} \quad (7)$$

$$\Delta E(k_s) = E(k_s) - E(k_s - 1) \quad (8)$$

Where $P_{ph}(k_s)$ and $V_{ph}(k_s)$ are respectively the power and voltage of the PV generator.

The value $E(k_s)$ shows whether the operating point of the load used at the time k_s is located on the left or right side of the maximum power point on the curve characteristic P (V). The value $\Delta E(k_s)$ expresses the direction of movement of this point.

The method chosen for inference in our work is that of Mamdani. As for defuzzification, it is the center of gravity method for the calculation of the output, the duty cycle of the DC/DC converter that has been preferred:

$$\alpha = \frac{\sum_{j=1}^n \mu(\alpha_j) - \alpha_j}{\sum_{j=1}^n \mu(\alpha_j)} \quad (9)$$

Table 1 shows the MPPT controller's inference matrix;

With:

PB (Positive Big).

PS (Positive Small).

ZE (Zero).

NS (Negative Small).

NB (Negative Big).

The choice of this classification is based on the reasoning where we'll work on two or more phases of tracking. The first phase is a tough phase where a significant research is used to accelerate the search and increases the response time. Once the operating point near the fuzzy algorithm MPP works in the fine phase where the research is low, which will reduce the amplitude of waves and thus will improve system efficiency.

We chose the Mamdani method as a method of fuzzy inference with (MAX-MIN operation). It is to use the MIN operator for AND, the MAX operator for OR.

The Center of gravity method is used for diffuziffication.

The batteries are very sensitive elements and their destruction easy. In what follows we propose an intelligent battery charger fuzzy type.

C. Battery Charger fuzzy type

We propose in this paper a battery charger fuzzy type that contains two inputs and two outputs, the scheme is focused on the Fig. 9;

Such as:

V_{BB} Battery voltage [V].

ΔV_{BB} Variation of battery voltage.

$K1$ Control signal of Switch 1 between the generator and the battery [0,1].

$K2$ Control signal of Switch 2 between the battery and the load [0,1].

Table 2 shows the matrix inference of the battery's controller;

The center of gravity method is used for diffuzification

V. APPLICATION AND DISCUSSION

Simulation models have been developed to verify the system performance under different scenarios using practical load profile and meteorological data. Simulation results are given and discussed.

A question arises, what regulator to choose? To resolve a comparative performance test is necessary, if only for the two most common technologies, namely the fuzzy controller and the P&O controller.

Fig. 10 below shows the variation of the power and voltage of the PV panel, power and battery voltage and the duty cycle of the two controllers fuzzy MPPT and P&O MPPT, under constant conditions: temperature = 25 °C and irradiation = 1,000 W/m², for a sampling frequency of 100 Hz.

Performance that presents the fuzzy control versus the P&O command lies partly in the speed to estimate the PPM without oscillations, and obtaining a maximum power of oscillation free, on the other hand.

For the two controllers, the voltage delivered to the load/battery appears to be greater than the acceptable voltage. A problem to be solved later through a voltage regulator. Fig. 11 shows an enlargement of the steady state characteristics of the Fig. 10 to clearly scrutinize the behavior of each command;

The fuzzy control reacts with delicacy avoiding any possible oscillation, at the same time all the features from the P&O MPPT experiences strong oscillations. In this case, the oscillations that duty cycle manifests have a direct impact on power efficiency, mainly due to its divergence and tilting the operating point beyond the real MPC.

Indeed, at the steady state the value of the power of fuzzy controller stabilizes at about 62.12 W, this value represents exactly the MPP studied under standard conditions panel. This means that the mechanism has really followed the maximum power point. While the power curve of the P&O controller exhibits oscillations in the shape of two peaks in opposite directions leading to a decrease in output power, which explains their location under the point 62.12 W, simply meaning that maximum power is never reached.

This result is a direct consequence of the approximation of continuous derivative by a discrete difference, which makes it impossible to cancel the derivative. In what follows, we study the influence of the sampling

frequency on the behavior of both controllers, through the power of the PVG. The frequency is 1,000 Hz. The result that follows is focused on the Fig. 12;

Changes in the sampling frequency do not affect the fuzzy controller. It keeps in fact a stable value of the power panels and logically proper duty cycle value.

However, as for the P&O controller, we won in response time of the system but lost not only as the signal power is all the more ripples in the case of a sample frequency of 100 Hz but also in computation time.

A. Operating mode in constant conditions

The purpose of these simulations is to visualize the operating point shift from MPP point. It is also used to assess the losses due to oscillations around this point. Fig. 13 below summarizes the results from the fuzzy control worn on the Fig. 10.

Based on these results, we observe that the MPPT algorithm using fuzzy logic is effective. Response times (transients) are acceptable. To better show the contribution of MPPT controller, we illustrate through Fig. 14 below the superposition of the output power characteristic of the PVG, pre- and post-pursuit;

The effect of the controller can be clearly seen in the sustaining power of PVG to its maximum value of 62.12 W, which is not the case for the passive system.

Fig. 15 gives the P-V and P-I characteristics of the controlled PVG under standard conditions;

Fig. 15 shows that the MPPT controller looks in the right direction and reached easily and directly to the PPM, which is located at 62.12 W, corresponding to $V_{max} = 20.19$ V and $I_{max} = 18.46$ A (for the entire generator and thus 3.07 A for the single module), set by the regulation $\alpha_{opt} = 0.34$.

And to test the effectiveness of the MPPT algorithm used in the photovoltaic system with respect to different environmental conditions, we decided for robustness test.

B. Robustness tests: Operating under varying conditions

1) Responses to varying irradiation conditions:

a) Sudden change of irradiation:

For a temperature of 25 °C, we study the system response to a sudden change of staggered illumination of 400 to 1,000 W/m². The results are shown in Fig. 16;

The fuzzy control has a good estimate to control without oscillations, which gives a fineness to the form of the power signal. The graphs above show the robustness of our MPPT controller.

b) Gradual variation of irradiation:

• Rapid increase in irradiation

The irradiation increases from 400 to 1,000 W/m² in a period of 5 s, the temperature is kept constant at 25 °C. The test results are recorded in Fig. 17 -a);

- *Slow increase of irradiation*

In this test, the irradiation from 700 to 1,000 W/m² in the space of 35 s, at a constant temperature of 25 °C. The simulation results are as shown in Fig. 17 -b);

The fuzzy logic technique has the advantage of working on two modes: a hard mode and a fine mode once the maximum power point captured. Fig. 17 -a) illustrates clearly this phenomenon.

- *Rapid decrease of irradiation*

Given by the Fig. 18- a), the answer to a rapid decrease in the irradiation, from 1,000 W/m² to 400 W/m² at a temperature of 25°C.

The test results are shown on Fig. 18 -a).

- *Slow decline in irradiation*

A slow decline 1,000 to 700 W/m² of the irradiation in a range of 35 s in the temperature of 25 °C is simulated in the test.

Fig. 18- b) reports the results of this simulation;

2) Responses to varying temperature conditions:

In addition to the solar irradiation, the temperature of the solar cell is an important factor which influences the characteristics of the solar panel.

Because of the large thermal mass of the solar panel, the change in temperature is very slow or the gradient is very small compared to the gradient of the irradiation.

Rapid temperature changes are rarely caused. Thus, the temperature depends on the flow of solar radiation. In the case of strong irradiation, the temperature increases gradually until thermal equilibrium is reached, when in cloudy weather, the temperature decreases gradually

A rapid decrease in temperature may happen when rainstorms fall suddenly and usually a rapid increase in the temperature never occurs.

a) Sudden change of temperature:

In this case, it maintains constant illumination, equal to the standard value of 1,000 W/m², and the reaction system is studied to a sudden change of temperature, ranging from level 25 to 45 °C to reach 60 °C.

We find the test results in Fig. 19 below;

As with a-1), the fuzzy control reacts with delicacy avoiding all possible oscillations.

b) Gradual change in temperature:

- *Rapid temperature increase*

An increase in temperature from 25 to 50 °C during a period of 5 s and under irradiation of 1,000 W/m² is simulated in this test. The results of this test are related on the Fig. 20- a);

- *Slow increase in temperature*

We simulate in this test an of increase temperature from 25 till 35 °C during a period of 5 s and under irradiation of 1,000 W/m². The results are shown in Fig. 20- b);

- *Rapid decrease in temperature*

The system response to a rapid decrease in temperature from 50 °C to 25 °C in a period of 5 s, with irradiation of 1,000 W/m² is studied in this case.

The results are shown in Fig. 20- a);

- *Slow decrease of the temperature*

The system's response to a slow decrease in temperature ranging from 35 to 25 °C with irradiation of 1,000 W/m² and produced in a time of 35 s is studied in this case.

The results are shown in Fig. 21- b);

➤ Comments

We find that the fuzzy controller is robust and follows the set whatever irradiation changes. These results are acceptable in terms of system stability.

The controller tracks perfectly linear decrement of power during the rapid variation of solar insolation.

Its fine behavior is clearly evident in the end of the rapid decline of illumination.

The rapid change in temperature produces a decrease in the output power of the PVG compared to that recorded in its PPM, accompanied by a displacement of the latter, to be detected by the tracking mechanism (tracking) in order to compensate it by a slight increase (adjustment) of the duty cycle that knows a relatively large variation, explained by the hard mode of fuzzy controller.

However, the slow changes in atmospheric conditions cause large oscillations of the duty cycle during the transition period of insolation/temperature, because of the divergence of the order, without affecting the output power for the simple reason that the fuzzy control is based on two operation modes:

A hard mode and a fine mode once the maximum power point captured. These are introduced in order to reduce not only the time necessary for the prosecution but also the fluctuations of power.

The ripples in question may be caused because the operating point reaches the MPP moving point repeatedly, or even because of the significant change in an increment used. This is the result of the fuzzy rules when a large slope is detected.

To reduce this effect, we can reduce the excursion of the duty cycle interval, except that it would lead to increased response time with respect to sudden changes in weather conditions.

C. Voltage regulation of the battery

As shown in Fig. 10, the battery voltage exceeds the rated voltage.

A battery charger fuzzy-type is proposed for the purpose of protecting the battery from the standalone installation. Fig. 22 demonstrates the effectiveness of that control in a variable insolation under the standard temperature of 25 °C;

When the irradiation changes, the voltage supplied to the load varies in the range $(21,6 \div 25)$ V. The regulator fully fulfills its role as it maintains the tension in a range that protects the battery.

VI. CONCLUSION

There are many aspects of concern in hybrid systems which have a considerable impact on the overall performance. A key element is the battery, a component that accounts for an important portion of the system cost. In hybrid power systems, the state of charge undergoes irregular variations as the load and the charging power from the PV array fluctuate. However, the behavior of batteries under _typical hybrid charging conditions_ is not yet fully understood neither is the impact of a battery cycling strategy on its expected lifetime.

Thus from the above discussion it can be understood that the major reason for slow penetration of solar PV system is its high capital cost and low efficiency. Hence lot of R&D work must be carried out by the government in this field to find out an improved technology which operates at high efficiency and available at low cost. The above discussion also gives us the clear idea about various components of PV micro grid system and its economic feasibility in topography of rural area.

FURTHER WORK

In the future, a more detailed model of the photovoltaic module can be developed from the one presented in this work. The more detailed model may take into account the effect of shading or partial shadows on the operation of the module. Also the effects of scaling up the photovoltaic sources may be

investigated to determine the suitability for large scale deployment.

Different algorithms for maximum power control can be developed for application on other renewable energy sources such as fuel cells and wind power. Artificial neural network algorithms can be developed to improve the performance of the solar energy conversion function of the MPPT. Overall, the shift from conventional energy sources to alternative energy means a lot more work needs to be done to fulfill the desire to produce clean, affordable and sustainable energy.

REFERENCES

- [1] H. Nakayama, E. Hiraki, T. Tanaka, N. Koda, N. Takahashi, S. Noda, "Stand-alone photovoltaic generation system with combined storage using lead battery and EDLC", In: IEEE Conferences. 2008.
- [2] M. Gottschalg, H. Rysse, "Comparison of different methods for the parameter determination of the solar cell's double exponential equation", 14th European Photo-voltaic Science and Engineering Conference (PVSEC), Barcelona, Spain, 1997.
- [3] H. Knopf, "Analysis, simulation, and evaluation of Maximum Power Point Tracking (MPPT) methods for a solar powered vehicle", Master of Science in Electrical and Computer Engineering, Portland State University, 1999.
- [4] AN. Celik, "Long-term energy output estimation for photovoltaic energy systems using synthetic solar irradiation data", Energy 2003;28:479-93.
- [5] L. Alan, H. Richard, "Fundamentals of Solar Cells: Photovoltaic Solar Energy Conversion", Academic Press, Inc, New York, NY, 1983.
- [6] A. Goetzberger, VU. Hoffmann, "Photovoltaic solar energy generation", Berlin, Heidelberg, New York: Springer; 2005 [Chapitre 7].
- [7] Z.M. Salameh, M.A. Casacca, and A.W. Lynch, "A mathematical model for lead-acid batteries", IEEE Transactions on Energy Conversion, 7(1):93-98, March 1992

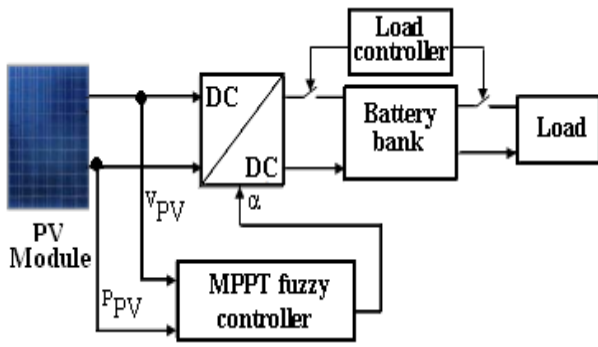


Fig. 1 Block diagram of proposed system

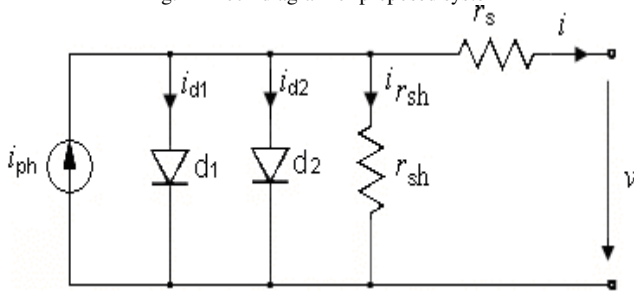


Fig. 2 Equivalent to two diodes of a photovoltaic cell model

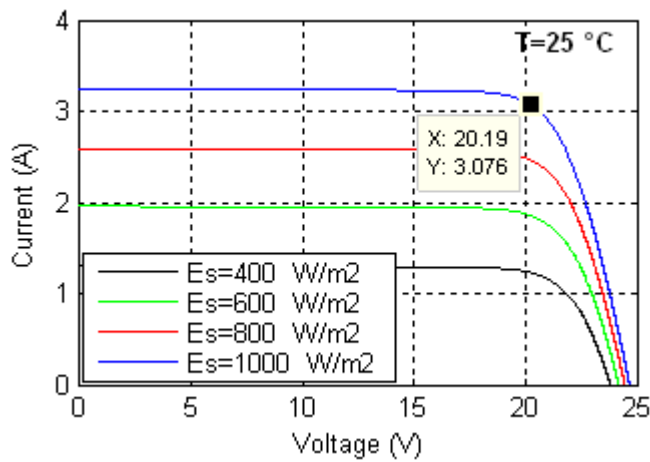


Fig. 3 Irradiation effect

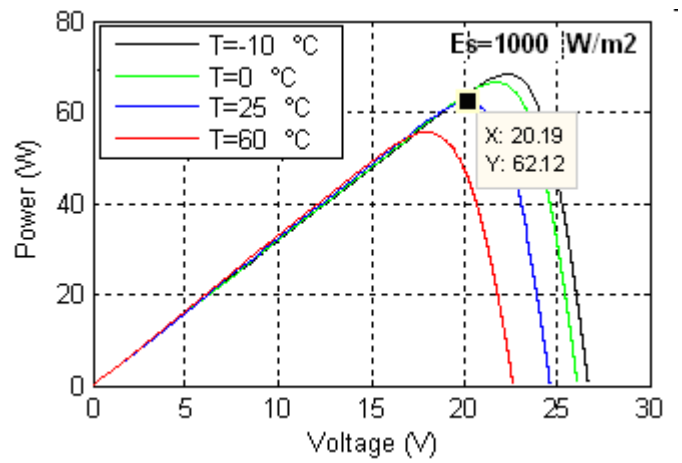
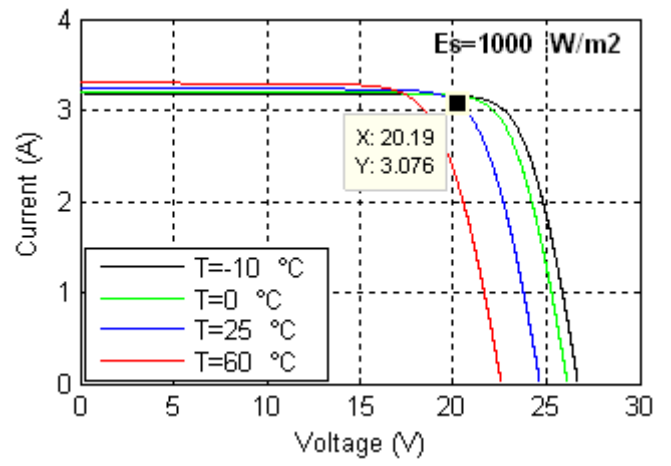
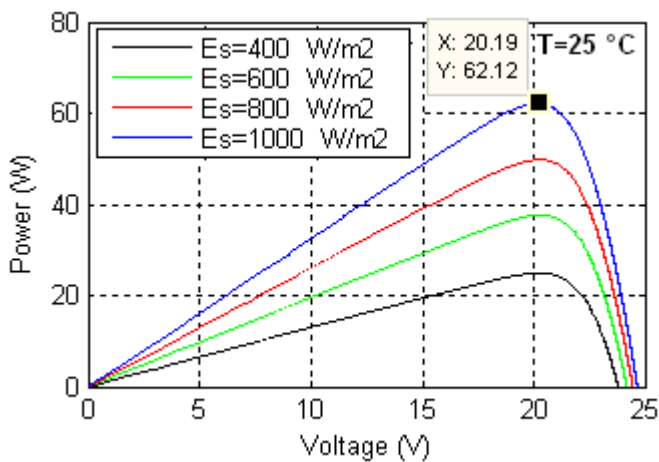


Fig. 4 Temperature effect

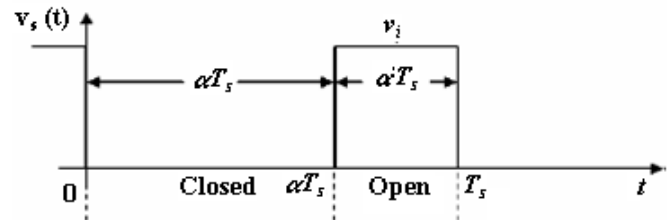


Fig. 5 Voltage $v_s(t)$ ideal of the switch, duty cycle d and switching period T_s

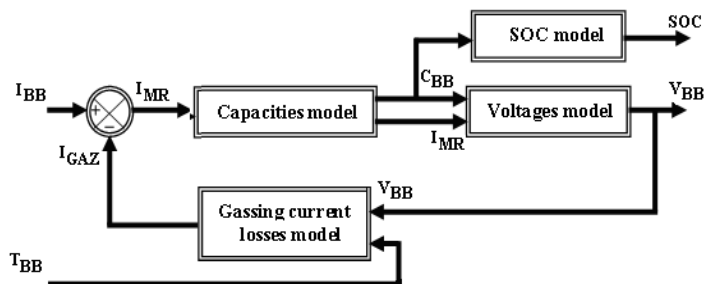


Fig. 6 Block diagram of a battery

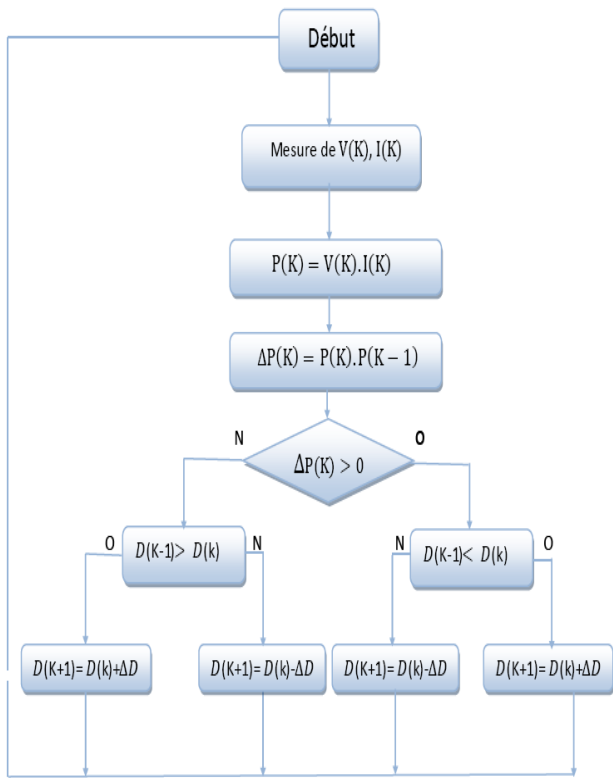


Fig. 7 Flowchart of Perturbation and Observation (P&O) algorithm

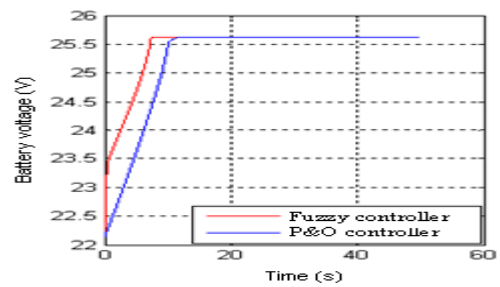
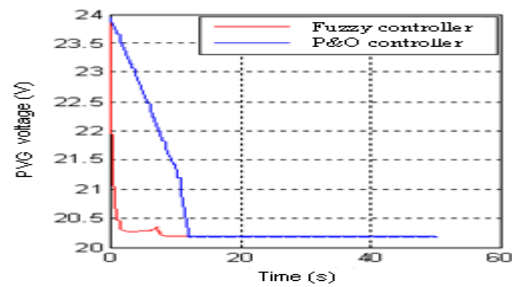
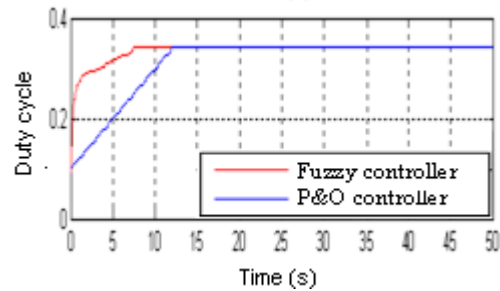
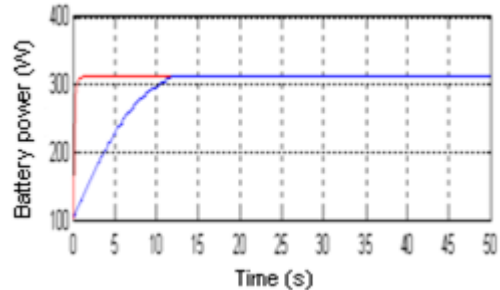
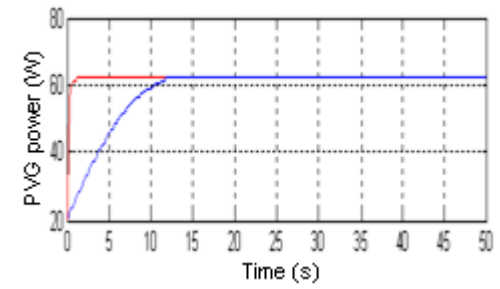


Fig. 10 Comparative performance test of the two MPPT Controllers, fuzzy and P&O one

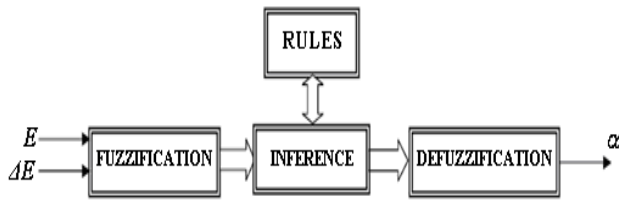


Fig. 8 Basic structure of the fuzzy controller

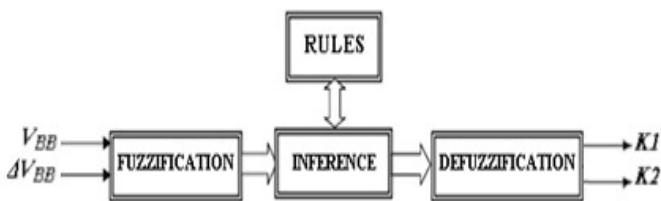


Fig. 9 Battery charger fuzzy type

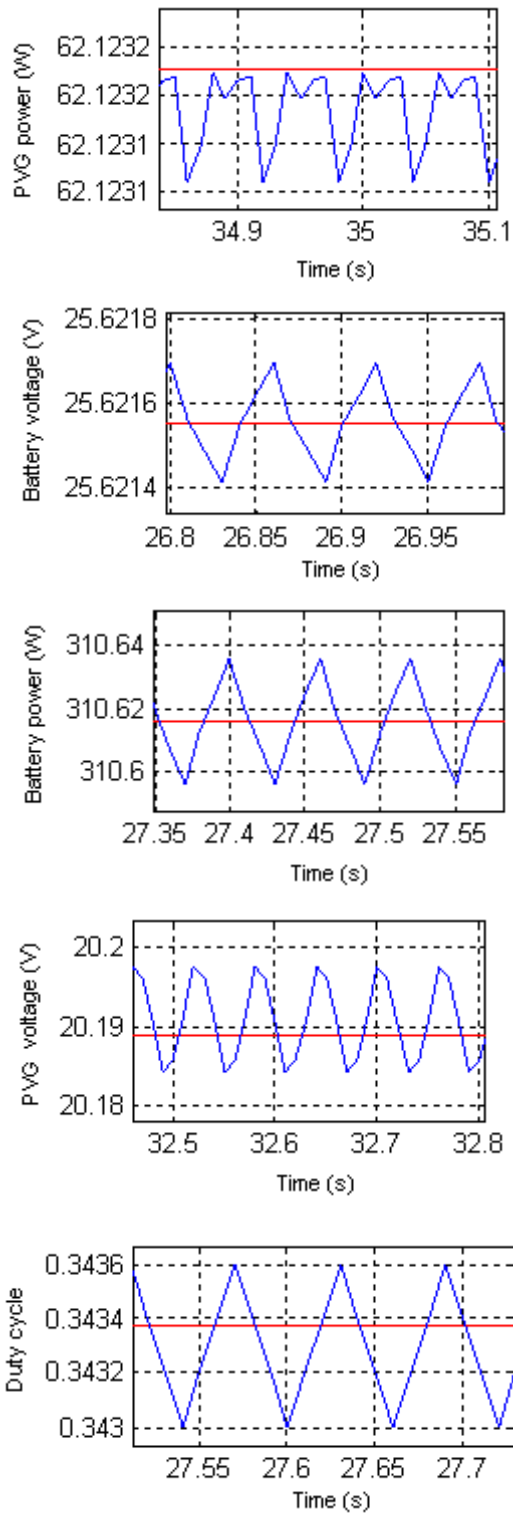
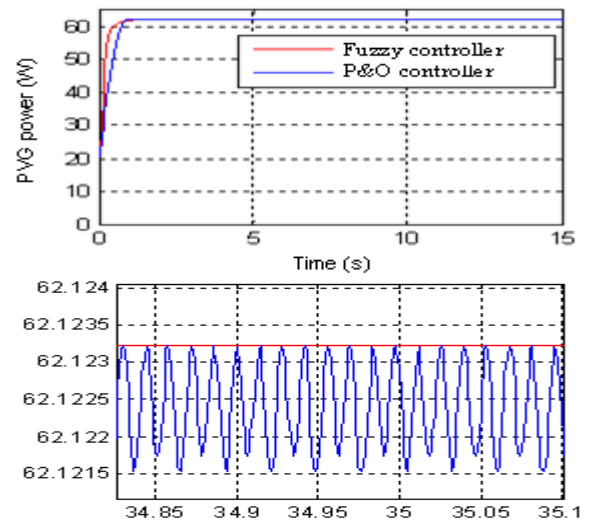


Fig. 11 Zoom of steady state characteristics of the Fig. 10



Zoom

Fig. 12 Influence of the sampling frequency on the behavior of the two controllers

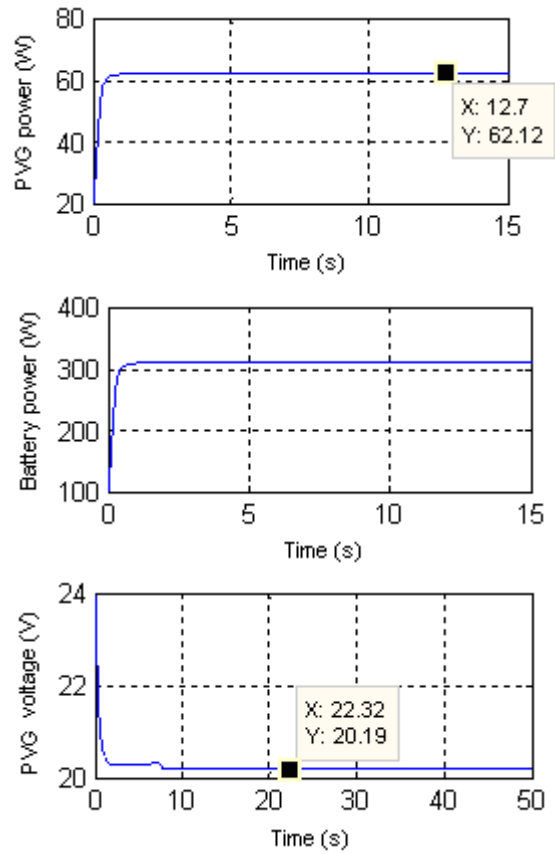
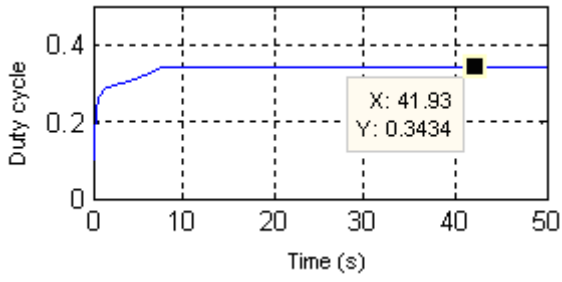


Fig. 13 Simulation results of the system under Standard Operating conditions



(pursuit) Fig. 13 Simulation results of the system under Standard Operating conditions

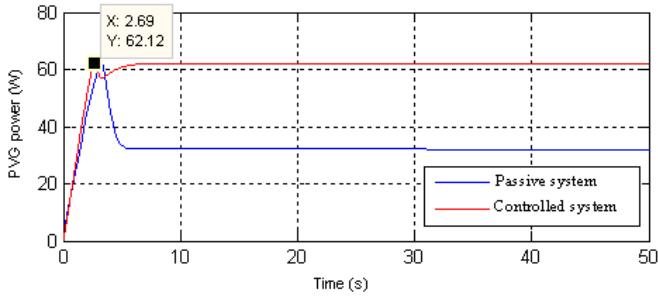


Fig. 13 PVG power pre- and post-pursuit

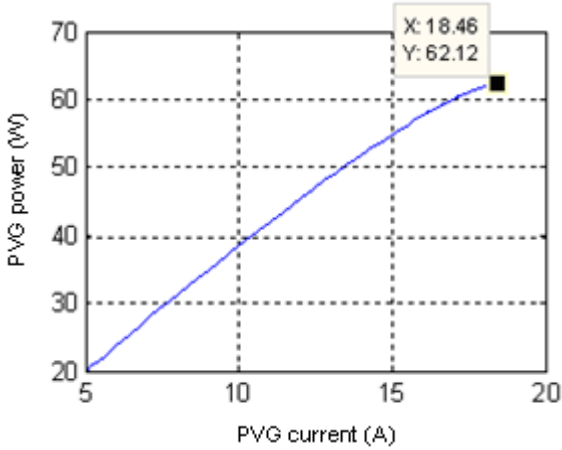
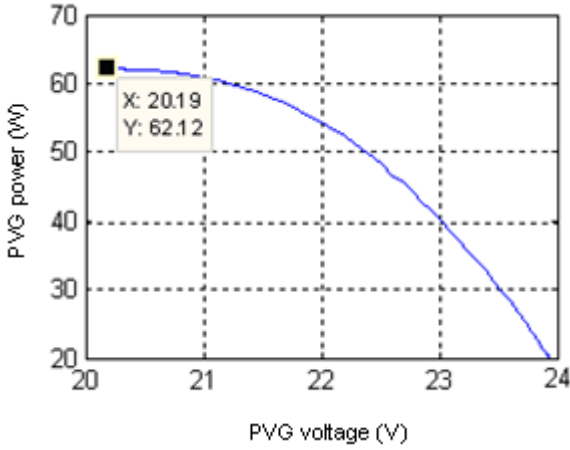


Fig. 15 Simulation curves of P-I and P-V characteristic of a PV panel controlled by the fuzzy MPPT controller, under constant conditions: temperature = 25 °C and irradiation = 1,000 W/m²

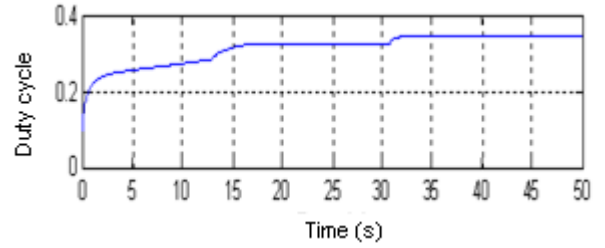
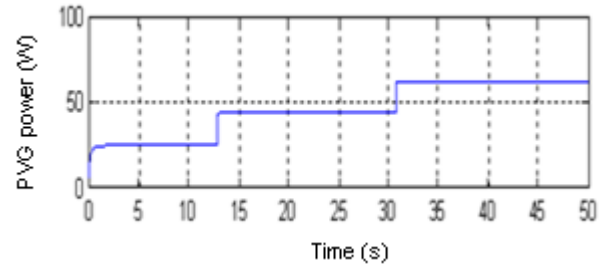
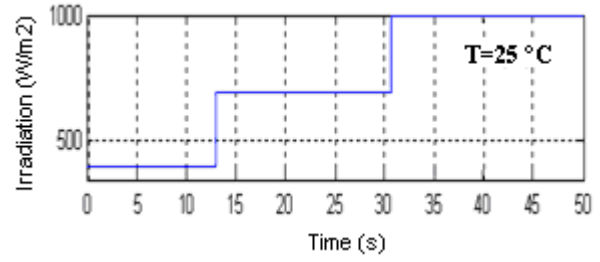


Fig. 16 Simulation results of the system under sudden change of irradiation

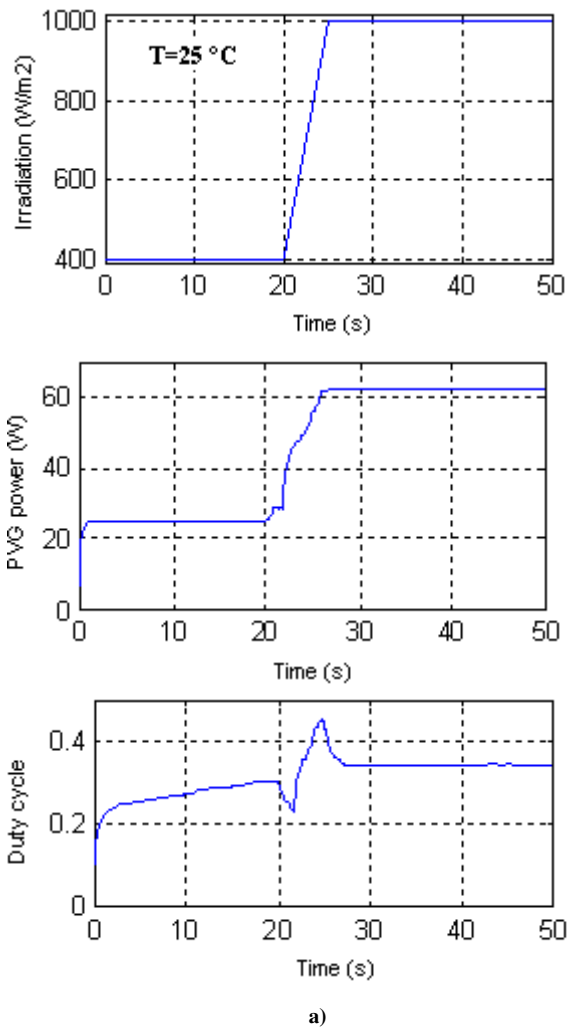


Fig. 17-a System response to a rapid increase in the irradiation

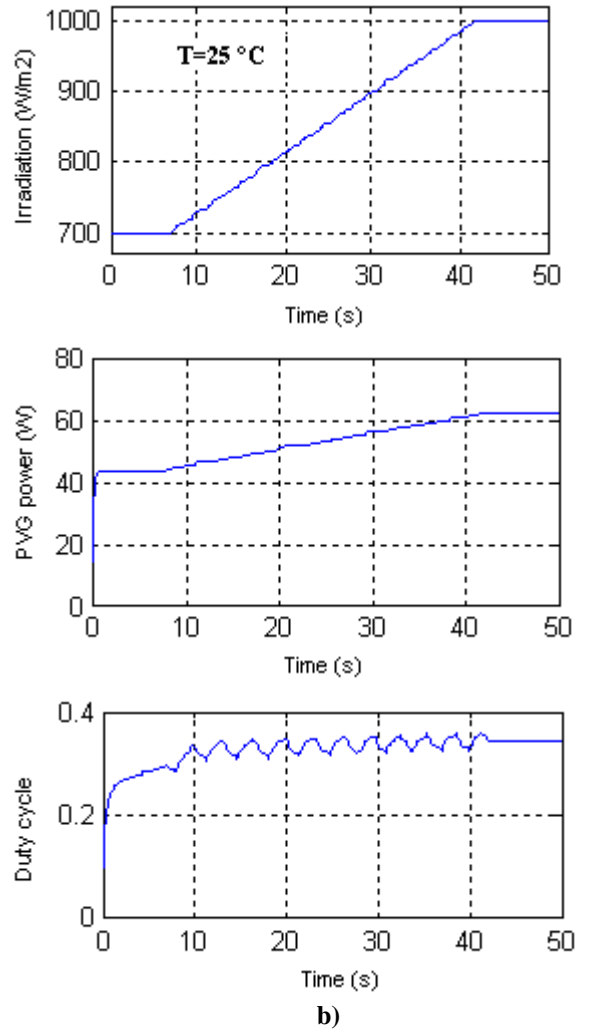
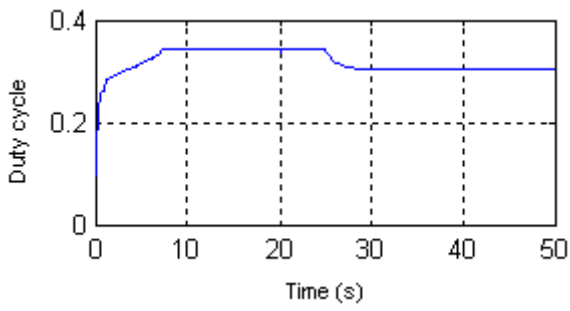
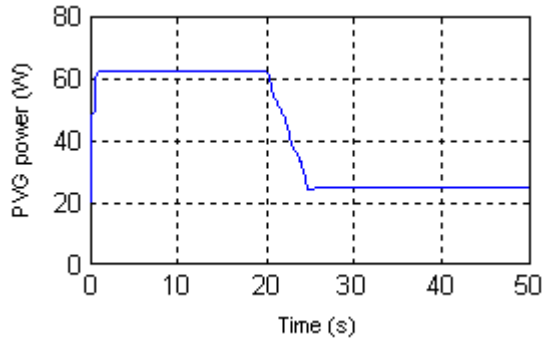
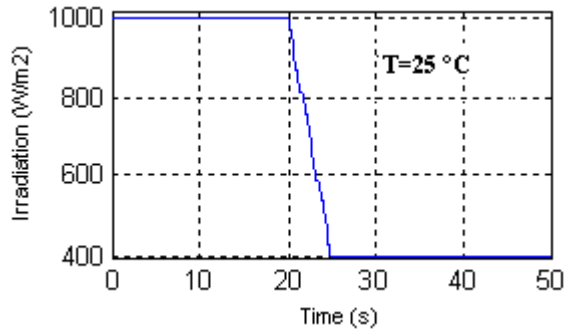
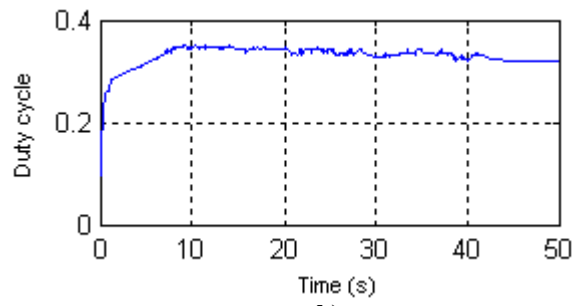
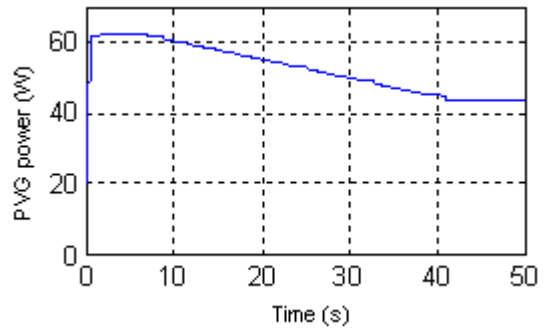
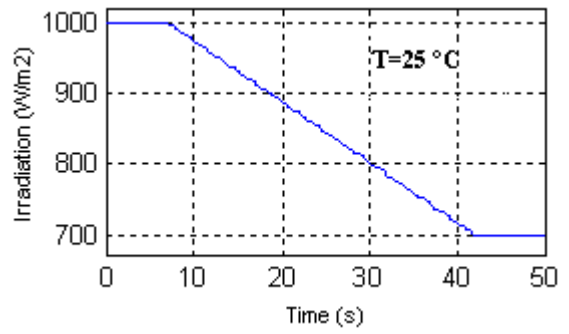


Fig. 17-b System response to a slow increase in the irradiation



a)

Fig. 18-a System response to rapid decreased irradiation



b)

Fig. 18-a System response to slow decreased irradiation

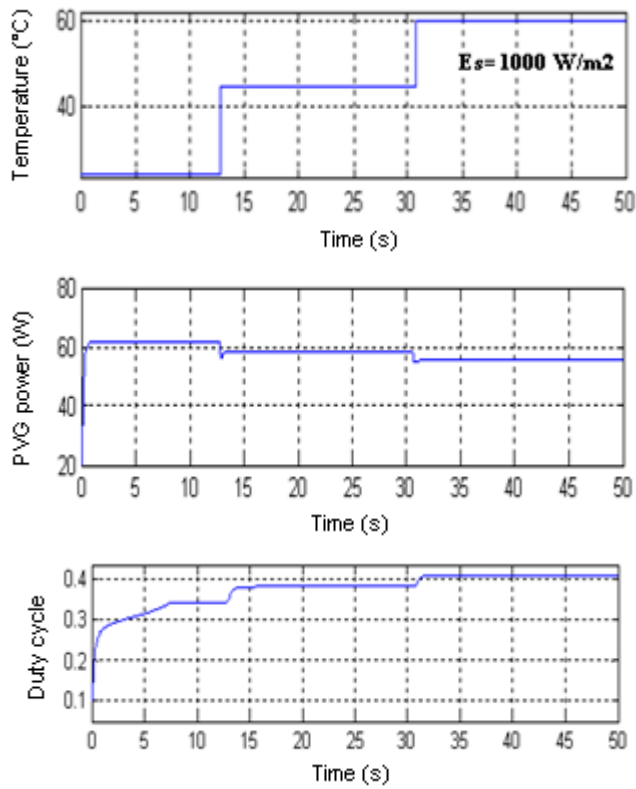


Fig. 19 Simulation results of the system under sudden variation of temperature

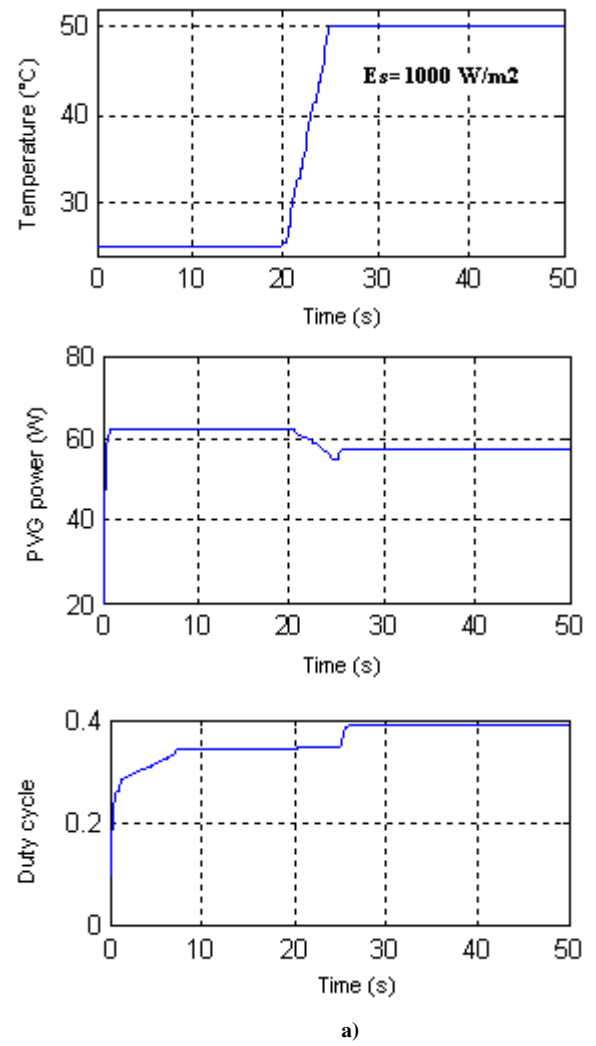
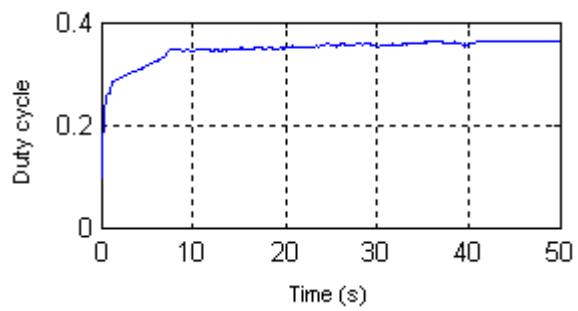
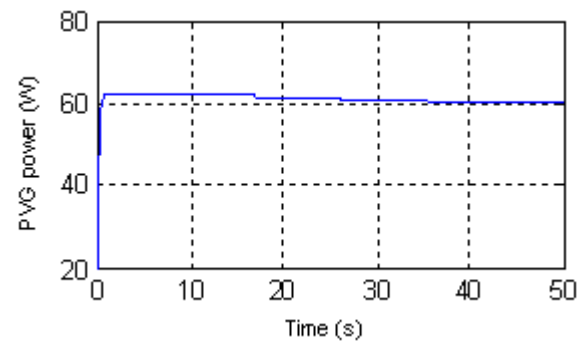
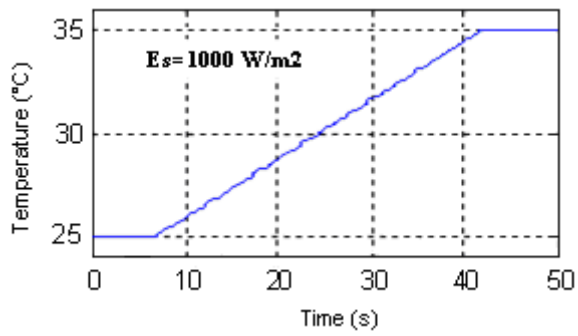
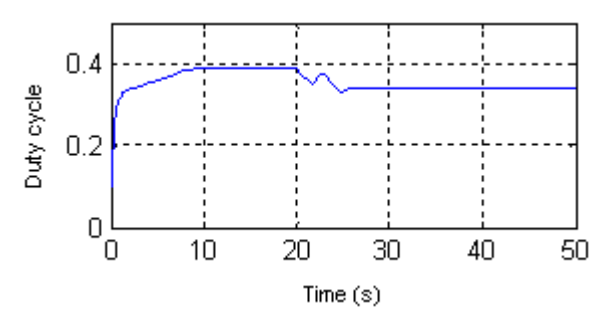
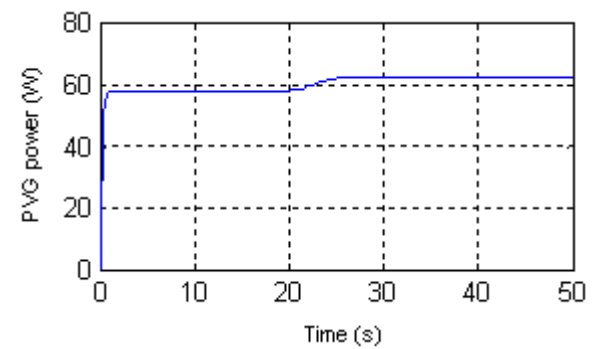
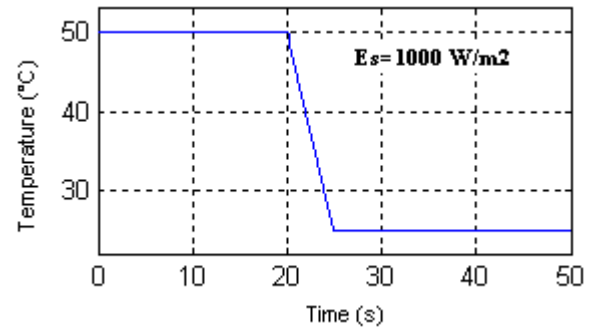


Fig. 20-a System response to a rapid increase in temperature



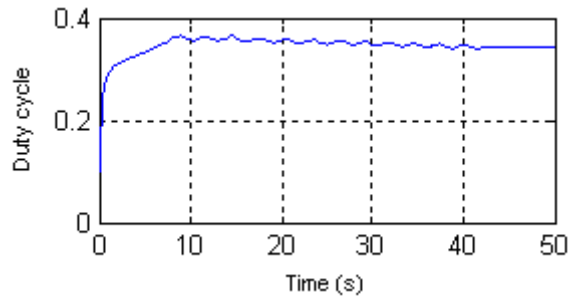
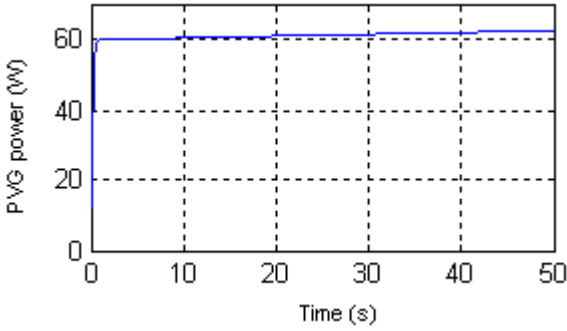
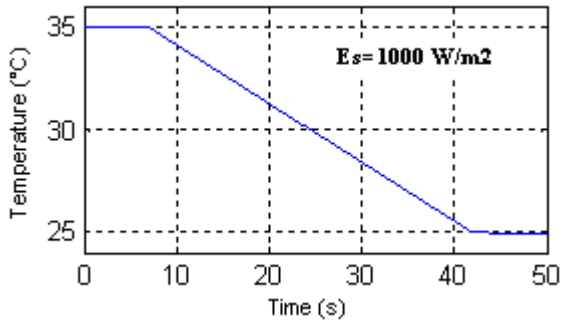
b)

Fig. 20-b System response to a slow increase in temperature



a)

Fig. 21-a System response to a rapid decrease in temperature



b)

Fig. 21-b System response to a slow decrease in temperature

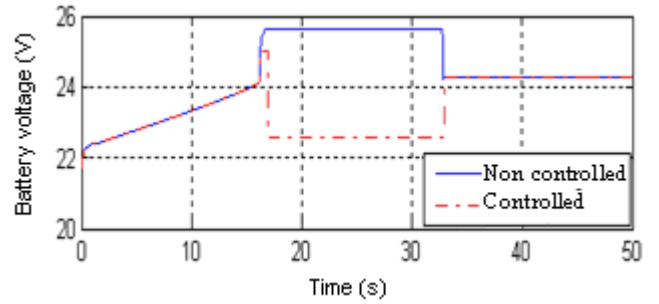
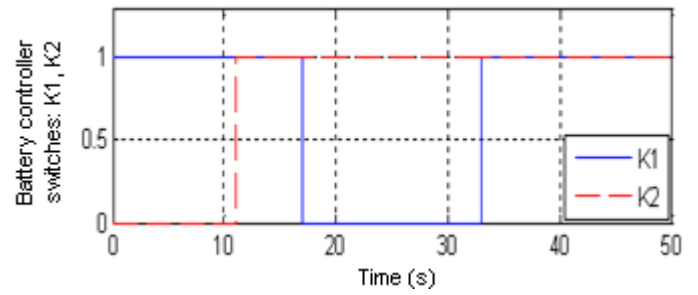
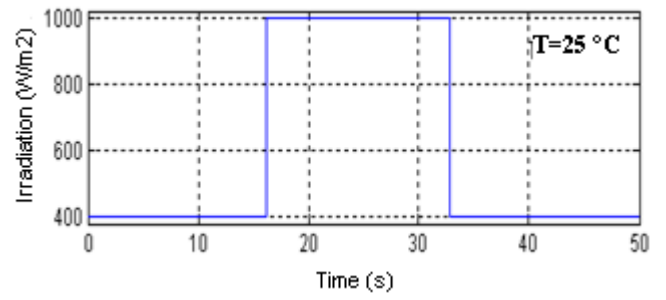


Fig. 22 Battery controller supply during a change of irradiation

TABLE I
MPPT CONTROLLER'S INFERENCE MATRIX

$E \downarrow \Delta E \rightarrow$	NB	NS	ZE	PS	PB
NB	ZE	ZE	PB	PB	PB
NS	ZE	ZE	PS	PS	PS
ZE	PS	ZE	ZE	ZE	NS
PS	NS	NS	NS	ZE	ZE
PB	NB	NB	NB	ZE	ZE

TABLE II
BATTERY'S CONTROLLER INFERENCE MATRIX

$\Delta E \downarrow E \rightarrow$	BTD	BD	BB	BC	BTC
EN	K1F K20	K1F $K20_{TEMP}$	K1F K2F	$K1F_{TEMP}$ K2F	K10 K2F
EZ	K1F K20	K1F K2F	K1F K2F	K1F K2F	K10 K2F
EP	K1F K20	K1F $K2F_{TEMP}$	K1F K2F	$K1 K10_{TEMP}$ K2F	K10 K2F